

13 Understanding Drought Awareness from Web Data

14 Mashrekur Rahman^a, Samuel Sandoval Solis^b, Thomas Harter^c, Mahmoud
15 Saeedimoghaddam^d, Niv Efron^e, Grey S. Nearing^f

^a*Department of Land, Air and Water Resources, University of California, Davis, One Shields Avenue, Davis, 95616, CA, USA*

^b*Department of Land, Air and Water Resources, University of California, Davis, One Shields Avenue, Davis, 95616, CA, USA*

^c*Department of Land, Air and Water Resources, University of California, Davis, One Shields Avenue, Davis, 95616, CA, USA*

^d*Department of Land, Air and Water Resources, University of California, Davis, One Shields Avenue, Davis, 95616, CA, USA*

^e*Google Research, 1600 Amphitheatre Parkway, Mountain View, 94043, CA, USA*

^f*Google Research, 1600 Amphitheatre Parkway, Mountain View, 94043, CA, USA*

16 **Abstract**

17 We used computer vision (U-Net) model to leverage Standardized Precipita-
18 tion Evapotranspiration Index (SPEI), Google Trends Search Interest (SI),
19 and Twitter data to understand patterns with which people in Continental
20 United States (CONUS) indicate awareness of and interest in droughts. We
21 found significant statistical relationships between the occurrence of meteorolo-
22 gical droughts (MD), as measured by SPEI, and SI on drought topics over
23 CONUS. SI tends to lag MD by a period of 2-3 months, however relationships
24 between MD and corresponding SI varies significantly over the CONUS in
25 both space and time. People in states with increasingly dry conditions have
26 become increasingly interested in drought topics. However, with worsening
27 drought conditions in California, public SI on drought topics in the state
28 has not increased significantly between 2016 and 2020, despite the overall SI

29 being high. We additionally applied sentiment analysis on 5 million tweets
30 related to droughts and found that public emotions towards drought have
31 become more polarized.

32 *Keywords:* Droughts, Image Segmentation, Google Trends, Twitter, SPEI,
33 Machine Learning

34 **1. Introduction**

35 Economic damage caused by droughts in the United States is estimated
36 to be in the billions of dollars [1]. Public perceptions and attitudes towards
37 droughts – both pre- and post-drought – are indicators of public reception
38 of water management and conservation measures [2, 3]. Adams et al. [4] as-
39 sessed the influence of attitudes and perceptions regarding multiple factors on
40 water conservation use in nine U.S. states and found that public perception
41 of the importance of water resources management significantly influenced wa-
42 ter conservation outcomes. A study on the sociological impacts of drought
43 perception in South-Central Nebraska revealed that crop and livestock pro-
44 ducers were becoming increasingly concerned about water scarcity resulting
45 from droughts [5]. Similar concerns were shared by farmers in a study con-
46 ducted in the Jucar River Basin in Spain [6] and in South Africa [7]. After a
47 record breaking drought in Texas in 2011, residents were significantly more
48 concerned with water availability and water conservation [8]. A recent study
49 on two cities in Alabama found that public awareness of drought is signifi-
50 cantly dependent on geographic, physical, and social contexts [9]. They used

51 Google Trends data in addition to survey data and suggested that future
52 studies consider Twitter data to gain a more complete understanding of so-
53 cial responses to drought hazards. However, a Continental United States
54 (CONUS)-scale study of human-drought interactions using web data has not
55 been conducted.

56 Evaluating public responses based upon questionnaire surveys is expen-
57 sive, time consuming, and often constrained by small sample-sizes [10, 11]. In
58 addition, questionnaire responses can be hard to interpret because of social
59 context, such as, non-response or social-desirability biases [12, 13]. The rise of
60 internet use means that a wide array of data sources have become available to
61 researchers. Search trends and social media data, although not without their
62 own limitations, can help mitigate some of the issues with direct surveys. In-
63 ternet users encompass most demographics and social-economic groups from
64 large geographic ranges. In 2018, 92% of households in the United States had
65 at least one type of computer and 85% had a broadband internet subscription
66 [14]. This makes a geographical area such as the CONUS an ideal candidate
67 for a large-scale web-based study. Numerous previous studies (some examples
68 mentioned below) have used internet query data as a proxy for survey data
69 in a diverse range of research topics. Carneiro et al. [15] argued that Google
70 Trends Search Interest (SI) data has the potential to track disease activity
71 and outbreaks earlier than traditional surveillance systems. Yang et al. [16]
72 successfully used Google Insights, which provides time series data of weekly
73 search trends data, as a proxy for surveys to investigate large-scale seasonal

74 patterns of depression. Stephens-Davidowitz [17] argued that using Google
75 search interest data as a proxy for racial animus provides a more substan-
76 tial estimate of its impact on electoral outcomes compared to survey-based
77 approaches. Hong et al. [18] used internet search volume data from Google
78 Trends as a proxy for population interest in telehealth and telemedicine, and
79 Arora et al. [19] comprehensively discussed the versatility and potential of
80 using Google search engine data as a proxy for survey in population health
81 research. Mellon [20] emphasized that in addition to its obvious advantages
82 with spatial coverage, Google search data can also provide more frequent and
83 timely information compared to surveys, as search trends are measured on
84 a weekly basis, allowing for easier comparisons over time. Given the broad
85 use of SI data as proxies for survey data, we utilize SI as a proxy for people’s
86 awareness of and interest in Meteorological Droughts (MD).

87 *1.1. Research Questions*

88 In this paper, we address the following research questions:

- 89 • Do people respond to meteorological droughts by searching drought
90 terms on Google and is there a time lag between occurrence of meteo-
91 rological droughts and rise in people’s search interest in droughts?
- 92 • Does the relationship between MD occurrences and people’s SI exhibit
93 spatial variation across CONUS?
- 94 • Have people in meteorological drought hotspots become increasingly
95 interested in drought topics?

- 96 • How have people’s sentiments about drought changed over time?

97 Understanding the public’s responses and sentiment towards meteorolog-
98 ical droughts offers key insights for decision makers who can leverage these
99 insights for early warnings, public service announcements, or targeted water
100 conservation initiatives. Recognizing shifts in sentiments aids in tailoring ef-
101 fective messaging to communities. Such insights directly align with societal
102 objectives, notably, reducing water consumption.

103 **2. Methods**

104 In this section, we discuss the data-driven experimental approaches and
105 methods that we used to address the research questions outlined above.

106 To address the first research question, we first looked at variations in
107 SI across CONUS within a study period (2004-2020). We then explored
108 (non-linear) correlations between the occurrences of MD and people’s search
109 interest in drought topics. We investigated whether there is a temporal lag
110 between MD indices and a subsequent rise in SI. We addressed these questions
111 by using a machine learning models (trained on lagged data) to help uncover
112 nonlinear correlations at various temporal lags.

113 To answer the second research question, we tested for spatial variability
114 in statistical relationships between MD and public SI across CONUS. We
115 explored this variability at a state-level.

116 For the third research question, we analyzed whether public SI in drought
117 topics has increased in regions frequently affected by MD. We first observed

Table 1: Overview of data sources and availability

Data	Abbreviation	Source	Years Available	Years Used
Standardized Precipitation and Evapotranspiration Index	SPEI	spei.csic.es	1900-2020	2004-2020
Google Trends Search Interest	SI	Google Trends API (trends.google.com)	2004-Present	2004-2020
Tweets	NA	Twitter API (developer.twitter.com/en/docs/twitter-api)	2006-Present	2008-2020

118 distributions and trends of MD and subsequent public SI across CONUS and
 119 within individual states for our study period. We broke down this analysis
 120 into smaller time periods to look at drought hotspots and trends over shorter
 121 time spans.

122 To address the fourth research question, we leveraged a data set of five
 123 million tweets containing drought-related terms, with the aim of tracking
 124 changing sentiments towards drought over time. We achieved this by mea-
 125 suring the percentage of sentiments in people’s tweets about drought terms
 126 between 2008 and 2020.

127 *2.1. Data*

128 Table 1 summarizes the three data types used in this study, including
 129 where the data was sourced and the temporal periods that we acquired and
 130 used.

131 *2.1.1. Standardized Precipitation and Evapotranspiration Index (SPEI)*

132 We acquired meteorological drought data from 1900 to 2020 from the
 133 Standardized Precipitation and Evapotranspiration Index (SPEI) data set
 134 [21]. SPEI is calculated by taking the difference between total precipitation
 135 and total potential evapotranspiration (PET) over a given period of time
 136 (e.g., monthly). SPEI is a standardized index, meaning that it is expressed

137 in units of standard deviations calculated over local (per pixel) climatologies,
 138 making it possible to compare drought conditions from different locations and
 139 different time periods. Calculating SPEI involves the following steps:

1. Calculate the difference between precipitation (P) and reference evapotranspiration ($ET0$) for each month or time step:

$$D_i = P_i - ET0_i \quad (1)$$

140 where D_i is the difference between precipitation and reference evapotranspiration for the i -th month or time step, P_i is the precipitation for the i -th month or time step, and $ET0_i$ is the reference evapotranspiration for the i -th month or time step.

2. Calculate the climatic water balance for each month or time step:

$$WB_i = \sum_{j=1}^n D_{i-j+1} \quad (2)$$

144 where WB_i is the climatic water balance for the i -th month or time
 145 step, and n is the time scale (e.g., 3, 6, or 12 months).

3. Fit a probability distribution, such as the three-parameter log-logistic distribution with the Maximum Likelihood Estimation (MLE) method, to the climatic water balance values:

$$F(WB) = \frac{1}{1 + \left(\frac{WB-\alpha}{\beta}\right)^{-\gamma}} \quad (3)$$

146 where $F(WB)$ is the cumulative probability distribution of the climatic
147 water balance, and α , β , and γ are the distribution parameters that
148 need to be estimated.

4. Calculate SPEI by transforming the fitted probability distribution to a standard normal distribution:

$$SPEI = \Phi^{-1}(F(WB)) \quad (4)$$

149 where SPEI is the Standardized Precipitation Evapotranspiration In-
150 dex, Φ^{-1} is the inverse standard normal cumulative distribution func-
151 tion, and $F(WB)$ is the cumulative probability distribution of the cli-
152 matic water balance.

153 SPEI can be calculated for a variety of time periods, ranging from 1
154 month to 48 months. We use monthly data in our calculations. Positive
155 SPEI values indicate wetter conditions, while negative values indicate drier
156 conditions. We created monthly SPEI maps over CONUS between 2004 and
157 2020. Fig 1 shows an example of one of these SPEI maps.

158 2.1.2. Google Trends Search Interest (SI)

159 We acquired Google Search Interest (SI) data from Google Trends using
160 the Trends API. The Trends API allows programmatic access to Google
161 trends data and track the popularity of different topics over time and place.

162 Given a specific term or topic, T , and a time range from t_1 to t_n , the
163 search interest for T at each time point, t_i , is calculated as:

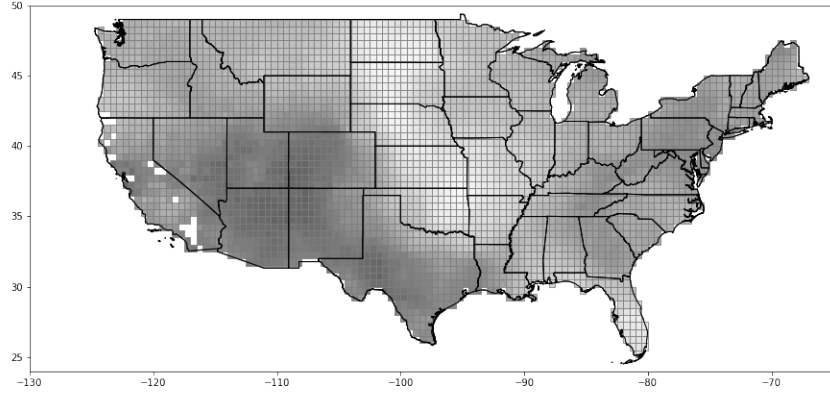


Figure 1: Example of a SPEI input map (Date: 08/16/2019). The image is in grayscale consistent with our actual input images.

$$SI(T, t_i) = \frac{S(T, t_i)}{S_{\max}(T)} \times 100 \quad (5)$$

164 where $SI(T, t_i)$ is the search interest for term or topic T at time point t_i ,
 165 $S(T, t_i)$ is the search volume for T at t_i , and $S_{\max}(T)$ is the maximum search
 166 volume for T within the specified time range. We use monthly state-wise SI
 167 data on “Drought” topic from 2004 to 2020 to create maps over the CONUS.
 168 Fig 2 shows an example of a Google SI target map.

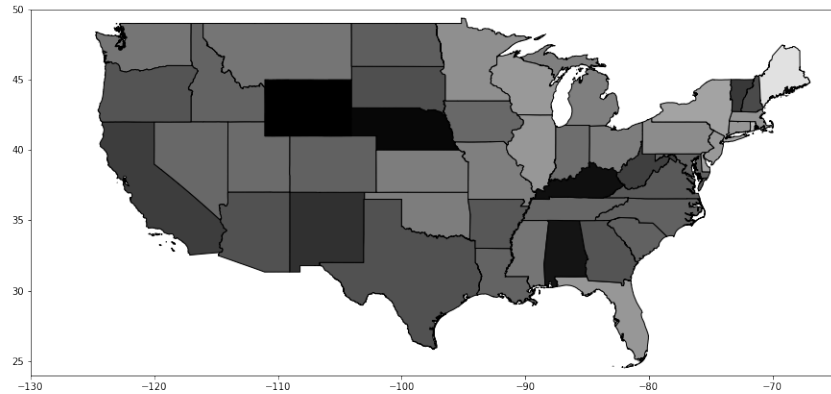


Figure 2: Example of a Google SI input map (Date: 08/2019). The image is in grayscale consistent with our actual target images into the model.

169 *2.1.3. Tweets*

170 We acquired Twitter data (Tweets) using the Twitter API. Our data set
171 consists of 5 million tweets related to the “Drought” topic from 2008 to 2020.
172 We use the Twitter data primarily for sentiment analysis. One thing to note
173 is that Twitter data is not geotagged, so our only option is to use global
174 tweets, but restricted to the English language.

175 *2.2. Analysis Methods*

176 *2.2.1. SI analysis*

177 To investigate how SI on droughts varies over CONUS, we first calculated
178 the state-wise average SI on drought terms within the period of our study,
179 and then rank states from highest to lowest values. We also calculated the
180 overall change in average state-wise SI to reveal where SI has risen the most.

181 *2.2.2. Relationship between MD and SI*

182 We used machine learning models to estimate non-linear relationship(s)
183 between MD and SI over CONUS. Specifically, we trained U-Net models [22]
184 to predict SI from SPEI maps. Details of our model architecture, training,
185 and evaluation are in Appendix Appendix A). In summary, we trained 6
186 models on 6 sets of lagged SPEI input maps (from 0 months lag to 5 months
187 lag) and the target data were their corresponding SI maps. Correlation be-
188 tween (out-of-sample) SI predictions made by these trained models and real
189 SI data is an estimate of the non-linear correlation between SPEI and SI at a
190 given lag time. We evaluated the models on time periods not used for train-
191 ing (training period: 01/01/2004 - 07/31/2017 and test period: 08/01/2017
192 - 12/31/2020) and report their corresponding performances as correlation
193 metrics.

194 *2.2.3. Spatial variability of the relationship between MD and SI*

195 We investigated spatial trends with respect to MD and corresponding
196 public engagement in terms of SI. We first used trained U-Net models to pro-

197 duce outputs of time series of SI estimates during a test period (08/01/2017
198 to 12/31/2020) for each individual pixel in the SPEI maps:

$$O_{a,b}(t) = U(T_{a,b}(t)) \quad (6)$$

199 where $O_{a,b}(t)$ is the U-Net output for pixel (a, b) at time t , $T_{a,b}(t)$ is the
200 input data for pixel (a, b) at time t , and U is the U-Net model function.

We then tested the model performance over time (using the coefficient of determination or R^2) for each individual pixel.

$$R_{a,b}^2 = R^2(O_{a,b}(t), G_{a,b}(t)) \quad (7)$$

201 where $R_{a,b}^2$ is the coefficient of determination for pixel (a, b) , $G_{a,b}(t)$ is
202 the ground truth (SI) data for pixel (a, b) at time t , and R^2 is the coefficient
203 of determination function. We then created a binary mask array based on
204 the geometry of CONUS and constructed heatmaps of the R^2 values. This
205 approach allows us to observe overall model performances over time across
206 CONUS, and also by individual states.

207 *2.2.4. Best lag times per state*

208 To investigate the existence of a temporal lag between occurrences of MD
209 and rise in public SI on droughts, we found the time lag that gives the best
210 SI predictions for each individual pixel. The different time lagged models
211 are named *0ml*, *1ml*, *2ml*, *3ml*, *4ml*, and *5ml*. To perform this analysis, we

212 followed these steps:

213 First, we calculated the highest R^2 value for each model:

$$max_r_squared_{a,b} = \max_{k=1}^6 R_{a,b,k}^2 \quad (8)$$

214 where $max_r_squared_{a,b}$ is the highest R^2 value for pixel (a, b) , and $R_{a,b,k}^2$
215 is the R^2 value for pixel (a, b) in model k .

216 Then we assigned each pixel with the highest R^2 value:

$$best_model_index_{a,b} = \arg \max_{k=1}^6 R_{a,b,k}^2 \quad (9)$$

217 where $best_model_index_{a,b}$ is the index of the model with the highest R^2
218 value for pixel (a, b) . Looking at this map, we can assess the best lag times
219 for each state.

220 2.2.5. Identifying MD hotspots over CONUS

221 We define MD hotspots as locations (SPEI pixels) that have been expe-
222 riencing (on average) abnormally dry or drought conditions over the past 16
223 years (2004-2020). The reasoning behind choosing this time period is be-
224 cause (i) it is the length of the existing Google Trends data that we have
225 available to apply our analyses on, and (ii) 16 years also encompasses a full
226 cycle of wet and dry conditions. To identify meteorological drought hotspots,
227 we performed the following steps:

228 We first calculated the average SPEI for the chosen period:

$$\overline{SPEI}_{a,b} = \frac{1}{N} \sum_{t=1}^N SPEI_{a,b}(t) \quad (10)$$

229 where $\overline{SPEI}_{a,b}$ is the average SPEI for pixel (a, b) over the whole study
 230 period (01/01/2004-12/31/2020), $SPEI_{a,b}(t)$ is the $SPEI$ value for pixel
 231 (a, b) at time t , and N is the total number of time steps within the chosen
 232 period (204 months).

233 In the next step, we normalize the $SPEI$ values:

$$SPEI'_{a,b} = \frac{\overline{SPEI}_{a,b} - \min(\overline{SPEI})}{\max(\overline{SPEI}) - \min(\overline{SPEI})} \quad (11)$$

234 where $SPEI'_{a,b}$ is the normalized $SPEI$ value for pixel (a, b) , and $\min(\overline{SPEI})$
 235 and $\max(\overline{SPEI})$ are the minimum and maximum average $SPEI$ values over
 236 CONUS, respectively. We generate a map of the meteorological drought dis-
 237 tribution over CONUS and deem areas with average $SPEI$ below zero to be
 238 drought hotspots.

239 *2.2.6. Exploring trends in MD hotspots*

240 To understand whether people in meteorological drought hotspots have
 241 become increasingly interested in droughts, we conducted a state-wise trend
 242 analysis on both yearly SPEI and SI data for the full study period of 2004-
 243 2020 and also breaking the analysis period to 2004-2010, 2011-2015, and
 244 2016-2020 to gain deeper insights into these trends. This involved fitting a
 245 linear regression model to the yearly SPEI and SI values for each state, and

246 extracting the slope of the fitted line as an indicator of the trend.

247 *2.2.7. Sentiment analysis on Twitter data*

248 We performed sentiment analysis on five million tweets related to drought
249 topics. Sentiment analysis allows us to understand the tone of human gen-
250 erated texts. We used VADER (Valence Aware Dictionary and Sentiment
251 Reasoner) – a lexicon and rule-based sentiment analysis tool that is specifi-
252 cally designed to work with social media data sets [23]. The overall sentiment
253 score (compound score) assigned to a tweet is a number between -1 and 1.
254 A score of -1 points towards a very negative sentiment while a score of 1
255 indicates a very positive sentiment. A neutral score of 0 indicates a neutral
256 sentiment. We calculated the per-year percentages of these three sentiments
257 within our tweet dataset and created a corresponding time series. Fig. 3
258 demonstrates an example of how a tweet about drought can receive a posi-
259 tive compound score (positive sentiment).

260 **3. Results and Analysis**

261 In this section we address the research questions laid out previously and
262 discuss the results of our analyses.

	author id	created_at	geo	id	lang	like_count	quote_count	reply_count	retweet_count	source	tweet	sentiment
9	2768501	2008-01-03 07:04:19+00:00		557555292	en	0	0	0	0	Twitter Web Client	NFF welcomes talks with Govt on drought assist...	pos

Figure 3: Positive sentiment assigned to a tweet about drought

263 *3.1. Do people respond to meteorological droughts by searching drought terms*
 264 *on Google and is there a time lag between occurrence of meteorological*
 265 *droughts and rise in people’s search interest in drought?*

266 The top 10 states by average SI over our study period were CA, NM, SD,
 267 CO, NE, WY, MT, ND, TX, and ID (Fig. 4). While the bottom 10 states
 268 were KY, LA, IL, TN, NJ, FL, OH, PA, NY, and MS. The top 10 states
 269 where people’s yearly SI rose the most between years 2004 and 2020 were
 270 NH, ME, VT, CA, OR, RI, CT, DC, MA, and IA.

271 Average R^2 for the statistical relationship between pixel values of target
 272 images and predicted pixel values by the U-Net models are shown in Fig. 5.
 273 The U-Net’s capacity for capturing nonlinear relationships is a key in this
 274 analysis. Results highlight significant nonlinear correlations between MD oc-

275 currences and associated anthropogenic response, as evidenced by variations
 276 in search interest across CONUS. It is also apparent that the 2ml and 3ml
 277 models (which represents the 2 months and 3 months lagged input images)
 278 with R^2 values of 0.61 and 0.62 demonstrated the strongest relationships -
 279 pointing towards the existence of a lag between occurrences of MD and rise
 280 in people's SI.

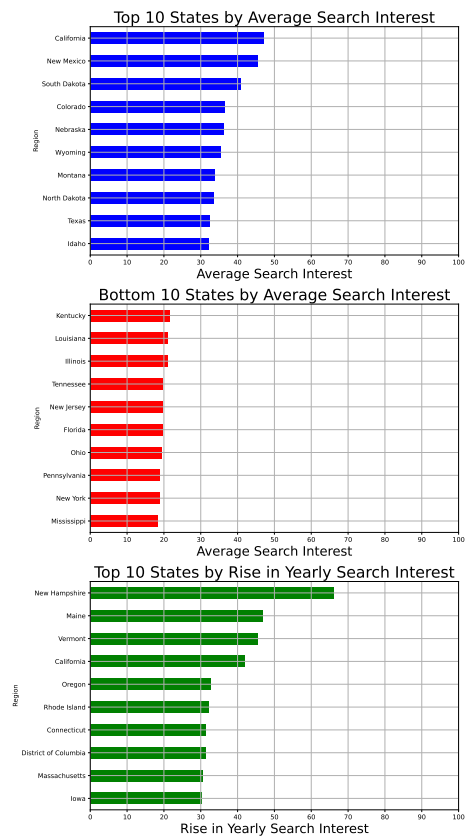


Figure 4: Results of the search interest analysis showing the top 10 and bottom 10 states in terms of the average search interest followed by the top 10 states by the rise in yearly search interest.

281 We generated a map of the best lag index (as explained in section 2.2)

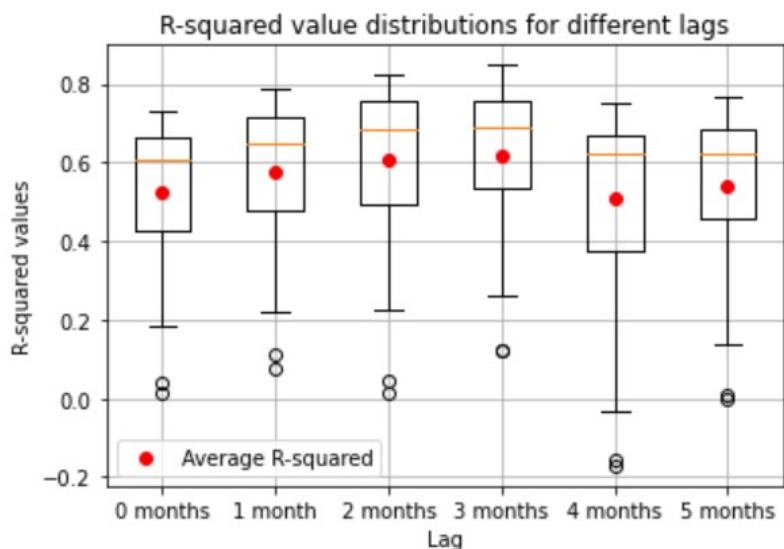


Figure 5: R^2 value distribution for different models - significant nonlinear correlations are found between MD occurrences and associated search interest across CONUS. The 2ml and 3ml models demonstrated the strongest relationships.

282 to obtain a snapshot of how the lag between occurrence of MD and rise in
 283 public SI in drought topics vary over CONUS (Fig. 6). We again observe that
 284 the 2ml and 3ml models (2 and 3 months lag) were the best performing lag
 285 models over CONUS. This indicates a clear existence of a lag variable which
 286 explains the delay between MD and rise in people's SI in drought topics in
 287 CONUS.

288 There are multiple factors which could drive a lag variable like this. We
 289 observe in Fig. 6 that regions with lag time less than or equal to 1 month
 290 generally rely on rain-fed irrigation (midwest and east coast) while states
 291 with lag times greater than or equal to 2 months mostly rely on water stor-
 292 age (surface reservoirs, aquifers) for irrigation. The types of crops grown and

293 water availability for irrigation (rain-fed or not) in these regions appear to be
 294 significant driving factors. Several studies have discussed the diverse impact
 295 of droughts and water scarcity on public reactions and opinions. For exam-
 296 ple, AghaKouchak et al. [24] argued that concurrent droughts and extreme
 297 heatwaves from climate change have significant social implications, and they
 298 could influence public opinions and reactions. Drier conditions are increas-
 299 ingly linked to public health issues [25, 26] and vegetation health as well
 300 [27, 28], which impact public perception of droughts and water availability,
 301 and subsequently, their interest in drought topics.

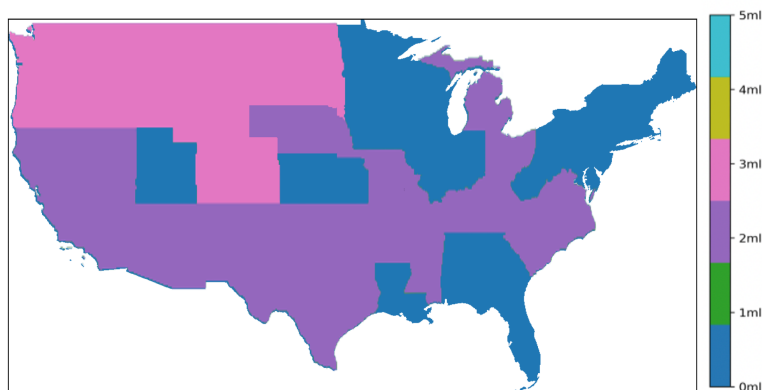


Figure 6: Distribution of best lag models over CONUS - 2ml and 3ml models (2 and 3 months lag) were the best performing models.

302 *3.2. Does the relationship between MD occurrences and people’s SI on drought*
 303 *topics demonstrate spatial variation across the CONUS?*

304 We calculated the time series of U-Net outputs during the test period and
 305 tested the model performances for each individual pixel (Fig. 7). Our results

306 show explicit spatial variation of the relationship between MD and public SI
307 on drought topics across CONUS.

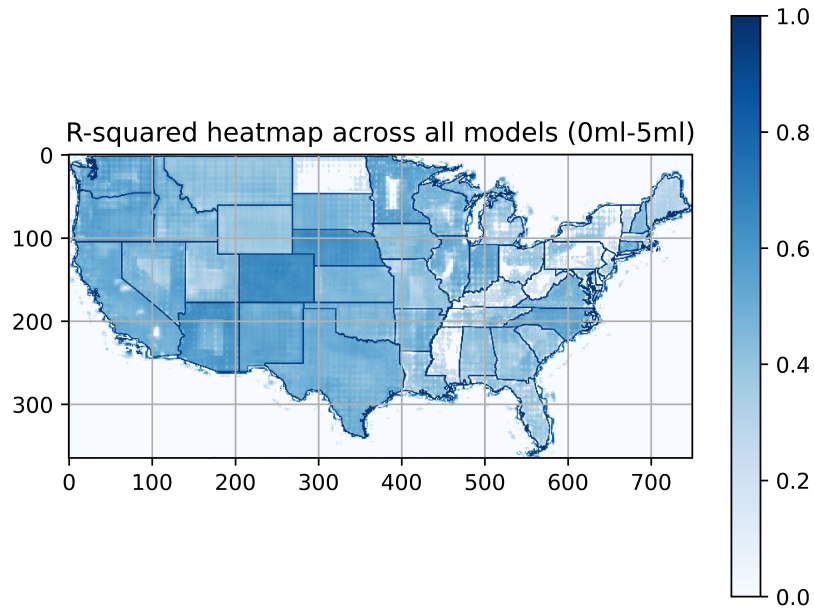


Figure 7: R^2 values averaged over the test period for CONUS and averaged across six models. Significant spatial variability can be seen in the relationship between MD and SI over CONUS.

308 State-level average test period R^2 values (across all the 6 models with
309 different lags) are shown in Fig. 8. Colorado, South Carolina, New Jersey,
310 and Nebraska had the highest average R^2 values, indicating that the SI of
311 their residents have varied significantly with local drought conditions over our
312 test period. On the other hand, CA, OR, NV, and ID had the lowest average
313 R^2 values, showing that the SI of their residents have not varied significantly
314 in drought topics with varying degrees of meteorological drought over our
315 test period.

316 Colorado has been in the midst of droughts (starting from 2000, with
317 severe drought affecting significant portion of the state between 2002-2004,
318 2012-2013, 2018-2019, 2020-2022)(droughtmonitor.unl.edu), and much of the
319 state has experienced water scarcity fueled by depleting snowpack [29] and
320 below average precipitation. South Carolina is also experiencing a drought,
321 mostly in the Upstate and Midlands, but the conditions are not as severe as
322 in Colorado. The drought in South Carolina has had an impact on agriculture
323 [30], recreation, and the environment (<http://www.scdrought.com/impacts.html>).
324 New Jersey has experienced abnormally dry conditions, but the state is
325 not in a drought. However, these conditions are affecting the environment
326 [31, 32, 30]. Nebraska has also experienced a moderate drought, with much
327 of the state experiencing abnormally dry or drought conditions, adversely
328 impacting agriculture and the environment [5, 33, 34]. The droughts in Col-
329 orado, South Carolina, New Jersey, and Nebraska are more recent compared
330 to states like California, Oregon, and Nevada. The drought in California
331 has been going on for over 20 years, while the drought trends in Colorado,
332 South Carolina, Nebraska have been increasing [35]. In the initial periods of
333 a prolonged drought, surface and groundwater reservoirs create a time buffer
334 between meteorological and anthropogenic drought. Perhaps people become
335 desensitized to drought topics after a certain period in a prolonged drought
336 - this may explain why SI is more correlated to meteorological droughts in
337 comparatively recently affected states during the model test period.

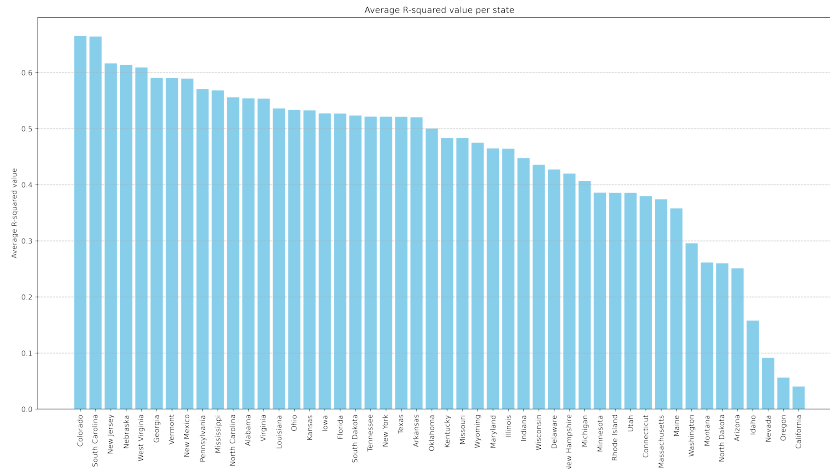


Figure 8: R^2 values (across the 6 models) for the relationship between MD and public SI in drought topics: Variation across the CONUS over the test period.

338 *3.3. Have people in MD hotspots become increasingly interested in drought*
 339 *topics?*

340 As described in section 2.2, we created a map to identify MD hotspots
 341 over CONUS between 2004-2020 (Fig. 9). We deem areas with average
 342 *SPEI* below zero to be drought hotspots. From the generated map, it is
 343 apparent that parts of WA, OR, CA, NV, AZ, UT, ID, NE, ND, SD, MT,
 344 CO, NM, TX, OK, MS, KY, OH, GA, FL, NC, SC, TN, NJ and parts of
 345 their surrounding states have become drought hotspots.

346 To investigate relationships between worsening droughts (decreasing *SPEI*)
 347 and increasing public SI at a state level, we conducted trend analyses on
 348 the entire study period. We found significant negative correlation ($r =$
 349 $-0.28, p\text{-value} = 0.0001$) in trends between states with decreasing *SPEI* and

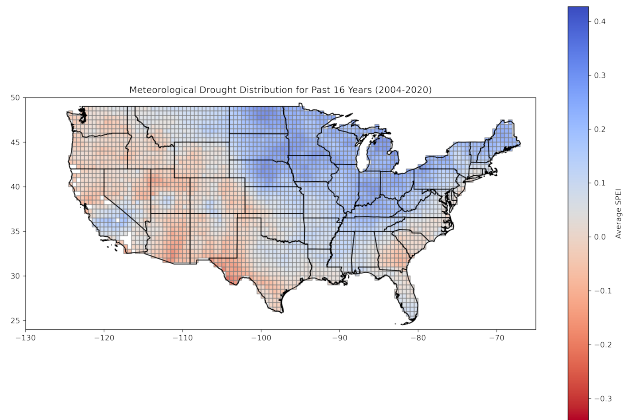


Figure 9: Drought hotspots in CONUS between 2004 and 2020.

350 increasing SI (Fig.10), indicating that people’s search interest has generally
 351 risen with increasingly dry conditions in these states.

352 We further broke down the trend analysis into smaller time periods to
 353 look at hotspots and trends over shorter periods (Fig. 11). For the state
 354 of California, we found that even though SPEI demonstrated a downward
 355 trend over the three periods, people’s SI has not trended upwards for the
 356 most recent time period (2016-2020) of our analysis.

357 These findings indicate that with worsening drought conditions in differ-
 358 ent CONUS states, public SI on drought topics also rose notably. Public SI
 359 trend in CA between 2016 and 2020 was not significant despite the drought
 360 conditions worsening over the previous 10 years. These observations warrant
 361 further insights into the underlying mechanisms driving these changes.

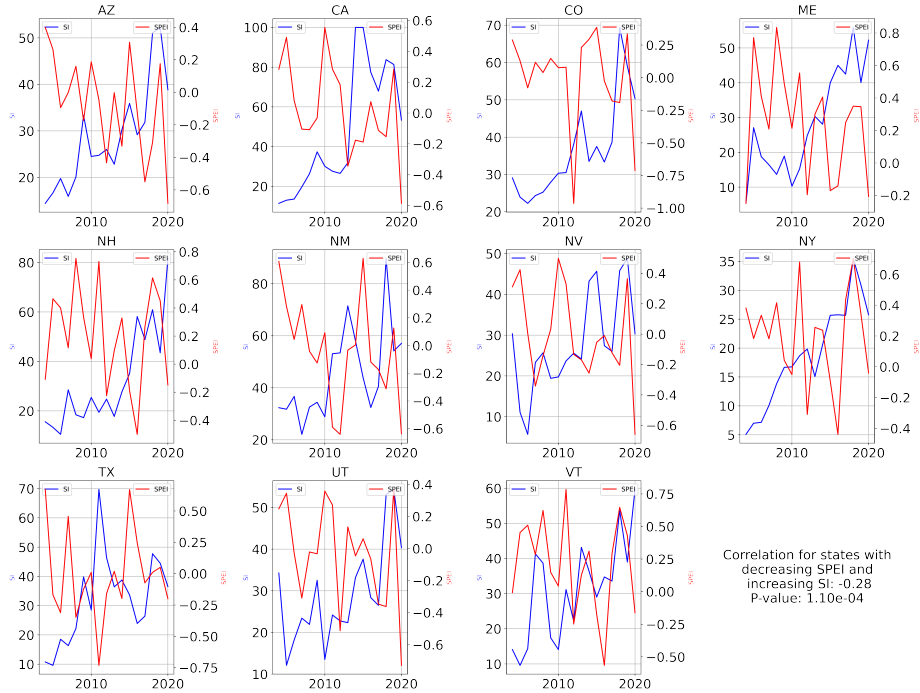


Figure 10: States with decreasing SPEI trends (left axis and red lines) and increasing SI trends (right axis and blue lines) between 2004 and 2020. Significant negative correlation ($r = -0.28, p - value = 0.0001$) was found between decreasing SPEI and increasing SI for these states.

362 3.4. *Have people’s reactions to drought become more polarized?*

363 As previously discussed in section 2.2, we apply sentiment analysis on
 364 five million tweets (containing drought terms). These tweets were not geo-
 365 tagged and therefore a representative of the global twitter community. Upon
 366 observing the variability of public sentiment, we find that both positive
 367 sentiment ($r = 0.24, p - value = 0.0018, BF10 = 12.36$) and negative sen-
 368 timent ($r = 0.24, p - value = 0.0017, BF10 = 12.91$) tweets have slightly
 369 trended upwards between 2004 and 2020. On the contrary, the percent-
 370 age of tweets with neutral sentiment have decreased ($r = -0.42, p - value =$

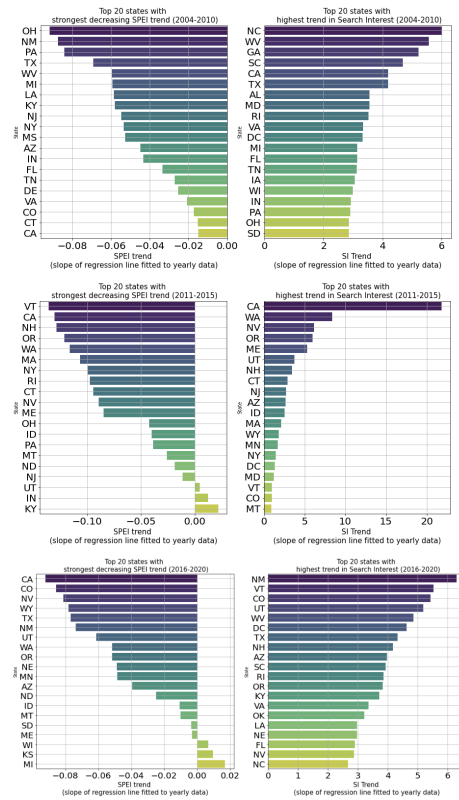


Figure 11: SPEI and SI trends by state (for top 20 states) broken down into three time periods: 2004-2010, 2011-2015, 2016-2020. For time period 2016-2020, people’s SI CA has not trended upwards for California despite the SPEI trending downward for the state over all the periods.

371 $9.95e - 09$, $BF10 = 1.21e + 06$) in relation to the positive and negative tweets
 372 over the same period (Fig. 12).

373 Our findings suggest that the public sentiments towards droughts may
 374 be becoming more polarized. This is likely due to multiple factors which
 375 could include increasing severity of droughts, increasing politicization of cli-
 376 mate change, increased regulations over groundwater to prevent groundwater
 377 overdraft, and spread of misinformation over the social media sphere. One

378 possible reason for these trends could be that as drought conditions worsen
 379 or become more prevalent, public awareness and concern grow, leading to
 380 more online searches and discussions about the topic. Positive sentiments
 381 could arise from discussions around successful drought management strate-
 382 gies, water conservation efforts, or community resilience. Negative sentiments
 383 might stem from the adverse impacts of droughts, such as crop loss, water
 384 shortages, and the associated socio-economic hardships. It can also be said
 385 that the rise in sentiment polarity is influenced by increasing public engage-
 386 ment with environmental issues more broadly. As discussions around specific
 387 environmental phenomena (like droughts) become increasingly popular, it is
 388 reasonable to think that they will become emotionally charged and polarized.

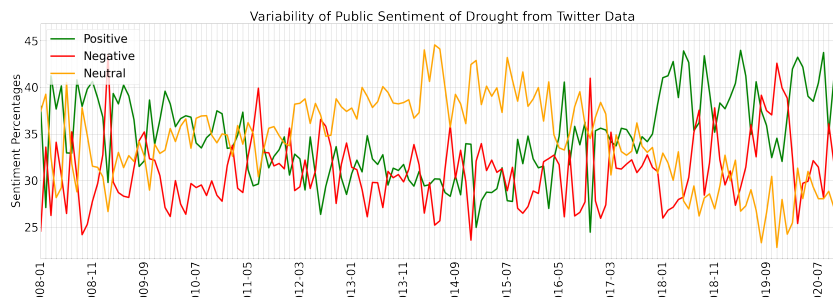


Figure 12: Variability of (global) public sentiment on drought topics in twitter and public search interest on droughts. Both positive sentiment and negative sentiment in tweets have slightly trended upwards between 2004 and 2020. On the contrary, the percentage of tweets with neutral sentiment have decreased

389 4. Conclusions & Discussion

390 We applied U-Net models to understand the relationships between MD
 391 and people’s interest in drought topics over CONUS. To do this, we leveraged

392 *SPEI*, Google Trends *SI*, and Twitter data. The primary findings of this
393 study are (see the four research questions outlined in Section 1.1):

- 394 • We found that people do respond to MD by searching Google for
395 drought-related topics. We found that correlations between *SPEI* and
396 *SI* were lagged at around 2 to 3 months with averaged R^2 values of *SI*
397 predicted from *SPEI* of > 0.6 .
- 398 • We found that relationships between MD and people's *SI* in drought
399 terms vary over CONUS. We found the strongest relationships in Col-
400 orado, South Carolina, New Jersey and Nebraska.
- 401 • We identified MD hotspots in the CONUS and found that *SI* in drought
402 topics have increased in states with worsening drought conditions. How-
403 ever, more recently (2016-2020), this effect was absent for California,
404 which has the overall highest *SI* and has been experiencing droughts
405 more or less consistently over the entire study period.
- 406 • Upon applying sentiment analysis to 5 million global drought-related
407 tweets, we found that people's reactions to droughts may be becoming
408 more polarized. This rise in polarity of emotions is happening alongside
409 increasing global public *SI* in drought topics (from Google Trends).

410 Our findings strongly point towards a lagged non-linear entanglement be-
411 tween the occurrence of MD and rise in people's awareness on drought topics
412 in the United States. Overall, public *SI* is notably higher and also increasing

413 in the regions with persistently dry or worsening drought conditions, ex-
414 cept recently for California. These observations provide impetus for future
415 studies investigating the underlying mechanisms driving human awareness of
416 droughts. For example, do people search less about droughts with changing
417 drought conditions as they become increasingly knowledgeable/aware over
418 time? We also encourage future studies to focus on the explanation of the
419 lag variable between occurrence of MD and rise relevant public SI - for ex-
420 ample, exploring how meteorological droughts impact agricultural, hydro-
421 logical, and socioeconomic droughts and quantifying the multidimensional
422 non-stationary interplay between these phenomena and their corresponding
423 human responses. The results of our study boosts the feasibility of train-
424 ing large-domain drought models in the sense that we provided the evidence
425 towards potential end-users/stakeholders.

426 As the impacts of anthropogenic-driven climate change become increas-
427 ingly felt and realized by humans across the world, we expect future exper-
428 iments to find more complex relationships between extreme weather events
429 (such as droughts) with people’s engagement on different platforms across the
430 global web. Given this scenario, computer vision models, such as our cus-
431 tom U-Nets, will continue to be significantly useful towards understanding
432 (evolving) human-drought interactions.

433 **5. Acknowledgements**

434 This study was supported by the Google Cloud Research Credits program
435 with the award GCP214472024.

436 The authors appreciate the cooperation from the Google Trends team for
437 providing access to Google Trends data through the Google Trends API.

438 The authors also appreciate the Twitter development team for providing
439 access to Twitter data through the Twitter API.

440 The code to reproduce all results and figures are available at
441 www.doi.org/10.5281/zenodo.8212808. Due to data and privacy restric-
442 tions, SPEI, Google, and Twitter datasets are not made publicly available.

443 **References**

- 444 [1] A. B. Smith, J. L. Matthews, Quantifying uncertainty and variable
445 sensitivity within the us billion-dollar weather and climate disaster cost
446 estimates, *Natural Hazards* 77 (2015) 1829–1851.
- 447 [2] H. E. Campbell, R. M. Johnson, E. H. Larson, Prices, devices, peo-
448 ple, or rules: the relative effectiveness of policy instruments in water
449 conservation 1, *Review of policy research* 21 (2004) 637–662.
- 450 [3] J. M. Clarke, R. R. Brown, Understanding the factors that influence
451 domestic water consumption within melbourne, *Australasian Journal of*
452 *Water Resources* 10 (2006) 261–268.

- 453 [4] D. C. Adams, D. Allen, T. Borisova, D. E. Boellstorff, M. D. Smolen,
454 R. L. Mahler, The influence of water attitudes, perceptions, and learning
455 preferences on water-conserving actions, *Natural Sciences Education* 42
456 (2013) 114–122.
- 457 [5] D. L. Woudenberg, D. A. Wilhite, M. J. Hayes, Perception of drought
458 hazard and its sociological impacts in south-central nebraska, *Great
459 Plains Research* (2008) 93–102.
- 460 [6] J. Urquijo, L. De Stefano, Perception of drought and local responses by
461 farmers: a perspective from the jucar river basin, spain, *Water Resources
462 Management* 30 (2016) 577–591.
- 463 [7] Y. Bahta, A. Jordaan, F. Muyambo, Communal farmers’ perception of
464 drought in south africa: Policy implication for drought risk reduction,
465 *International Journal of Disaster Risk Reduction* 20 (2016) 39–50.
- 466 [8] D. M. Gholson, D. E. Boellstorff, S. R. Cummings, K. L. Wagner, M. C.
467 Dozier, A survey of public perceptions and attitudes about water avail-
468 ability following exceptional drought in texas, *Journal of Contemporary
469 Water Research & Education* 166 (2019) 1–11.
- 470 [9] W. Shao, J. Kam, E. Cass, Public awareness and perceptions of drought:
471 A case study of two cities of alabama, *Risk, Hazards & Crisis in Public
472 Policy* (2022).

- 473 [10] S. McLafferty, Conducting questionnaire surveys, *Key methods in ge-*
474 *ography* 3 (2016) 129–142.
- 475 [11] J. J. Vaske, Advantages and disadvantages of internet surveys: Intro-
476 *duction to the special issue*, *Human Dimensions of Wildlife* 16 (2011)
477 149–153.
- 478 [12] R. J. Fisher, Social desirability bias and the validity of indirect ques-
479 *tioning*, *Journal of consumer research* 20 (1993) 303–315.
- 480 [13] R. M. Groves, Nonresponse rates and nonresponse bias in household
481 *surveys*, *Public opinion quarterly* 70 (2006) 646–675.
- 482 [14] M. Martin, et al., Computer and internet use in the united states: 2018,
483 *American Community Survey Reports*. Recuperado de [https://www.](https://www.census.gov/library/publications/2021/acs/acs-49.html)
484 [census.gov/library/publications/2021/acs/acs-49.html](https://www.census.gov/library/publications/2021/acs/acs-49.html) (2021).
- 485 [15] T. Carneiro, R. V. M. Da Nóbrega, T. Nepomuceno, G.-B. Bian, V. H. C.
486 *De Albuquerque*, P. P. Reboucas Filho, Performance analysis of google
487 *colaboratory as a tool for accelerating deep learning applications*, *IEEE*
488 *Access* 6 (2018) 61677–61685.
- 489 [16] A. C. Yang, N. E. Huang, C.-K. Peng, S.-J. Tsai, Do seasons have an
490 *influence on the incidence of depression? the use of an internet search*
491 *engine query data as a proxy of human affect*, *PloS one* 5 (2010) e13728.
- 492 [17] S. Stephens-Davidowitz, The cost of racial animus on
493 *a black candidate: Evidence using google search data*,

- 494 Journal of Public Economics 118 (2014) 26–40. URL:
495 <https://www.sciencedirect.com/science/article/pii/S0047272714000929>.
496 doi:<https://doi.org/10.1016/j.jpubeco.2014.04.010>.
- 497 [18] Y. Hong, J. Lawrence, D. Williams, I. Mainous, Population-level in-
498 terest and telehealth capacity of us hospitals in response to covid-
499 19: cross-sectional analysis of google search and national hospital sur-
500 vey data. *jmir public health surveill.* 2020 apr 07; 6 (2): e18961. doi:
501 10.2196/18961, ????
- 502 [19] V. S. Arora, M. McKee, D. Stuckler, Google trends: Opportunities
503 and limitations in health and health policy research, *Health Policy* 123
504 (2019) 338–341.
- 505 [20] J. Mellon, Where and when can we use google trends to measure issue
506 salience?, *PS: Political Science & Politics* 46 (2013) 280–290.
- 507 [21] S. Beguería, sbegueria/speibase: Version 2.7, 2022.
508 URL: <https://doi.org/10.5281/zenodo.5864391>.
509 doi:10.5281/zenodo.5864391.
- 510 [22] O. Ronneberger, P. Fischer, T. Brox, U-net: Convolutional networks
511 for biomedical image segmentation, in: *Medical Image Computing*
512 *and Computer-Assisted Intervention–MICCAI 2015: 18th International*
513 *Conference, Munich, Germany, October 5–9, 2015, Proceedings, Part III*
514 18, Springer, 2015, pp. 234–241.

- 515 [23] C. Hutto, E. Gilbert, Vader: A parsimonious rule-based model for senti-
516 ment analysis of social media text, in: Proceedings of the international
517 AAAI conference on web and social media, volume 8, 2014, pp. 216–225.
- 518 [24] A. AghaKouchak, L. Cheng, O. Mazdidasni, A. Farahmand, Global
519 warming and changes in risk of concurrent climate extremes: Insights
520 from the 2014 california drought, *Geophysical Research Letters* 41
521 (2014) 8847–8852.
- 522 [25] R. Barrera, V. Acevedo, M. Amador, M. Marzan, L. E. Adams, G. Paz-
523 Bailey, El niño southern oscillation (enso) effects on local weather, ar-
524 boviral diseases, and dynamics of managed and unmanaged populations
525 of aedes aegypti (diptera: Culicidae) in puerto rico, *Journal of Medical*
526 *Entomology* (2023) tjad053.
- 527 [26] E. Moyo, L. G. Nhari, P. Moyo, G. Murewanhema, T. Dzinamarira,
528 Health effects of climate change in africa: A call for an improved imple-
529 mentation of prevention measures, *Eco-Environment & Health* (2023).
- 530 [27] A. R. Chilakala, P. Pandey, A. Durgadevi, M. Kandpal, B. S. Patil,
531 K. Rangappa, P. C. O. Reddy, V. Ramegowda, M. Senthil-Kumar,
532 Drought attenuates plant responses to multiple rhizospheric pathogens:
533 A study on a dry root rot-associated disease complex in chickpea fields,
534 *Field Crops Research* 298 (2023) 108965.
- 535 [28] L. Bao, L. Yu, Y. Li, F. Yan, V. Lyne, C. Ren, Climate change impacts

- 536 on agroecosystems in china: Processes, mechanisms and prospects, Chi-
537 nese Geographical Science (2023) 1–18.
- 538 [29] A. J. Heldmyer, N. R. Bjarke, B. Livneh, A 21st-century perspective on
539 snow drought in the upper colorado river basin, JAWRA Journal of the
540 American Water Resources Association (2023).
- 541 [30] M. Noel, D. Bathke, B. Fuchs, D. Gutzmer, T. Haigh, M. Hayes,
542 M. Poděbradská, C. Shield, K. Smith, M. Svoboda, Linking drought
543 impacts to drought severity at the state level, Bulletin of the American
544 Meteorological Society 101 (2020) E1312–E1321.
- 545 [31] R. Mohammed, L. Maskal, Drought climatology and impacts in the
546 northeast: Case studies for new jersey and delaware, in: AGU Fall
547 Meeting Abstracts, volume 2021, 2021, pp. NH15F–0501.
- 548 [32] B. Johnson, M. Sukhdeo, Drought-induced amplification of local and
549 regional west nile virus infection rates in new jersey, Journal of medical
550 entomology 50 (2013) 195–204.
- 551 [33] A. M. Abadi, Y. Gwon, M. O. Gribble, J. D. Berman, R. Bilotta,
552 M. Hobbins, J. E. Bell, Drought and all-cause mortality in nebraska
553 from 1980 to 2014: Time-series analyses by age, sex, race, urbanic-
554 ity and drought severity, Science of the Total Environment 840 (2022)
555 156660.

- 556 [34] P. Nasta, J. B. Gates, Plot-scale modeling of soil water dynamics and
557 impacts of drought conditions beneath rainfed maize in eastern nebraska,
558 *Agricultural water management* 128 (2013) 120–130.
- 559 [35] D. L. Ficklin, J. T. Maxwell, S. L. Letsinger, H. Gholizadeh, A climatic
560 deconstruction of recent drought trends in the united states, *Environ-*
561 *mental Research Letters* 10 (2015) 044009.
- 562 [36] S. Minaee, Y. Boykov, F. Porikli, A. Plaza, N. Kehtarnavaz, D. Ter-
563 zopoulos, Image segmentation using deep learning: A survey, *IEEE*
564 *transactions on pattern analysis and machine intelligence* 44 (2021)
565 3523–3542.
- 566 [37] D. Qin, J. Yu, G. Zou, R. Yong, Q. Zhao, B. Zhang, A novel combined
567 prediction scheme based on cnn and lstm for urban pm 2.5 concentration,
568 *IEEE Access* 7 (2019) 20050–20059.
- 569 [38] H. Hasan, H. Z. Shafri, M. Habshi, A comparison between support
570 vector machine (svm) and convolutional neural network (cnn) models for
571 hyperspectral image classification, in: *IOP Conference Series: Earth and*
572 *Environmental Science*, volume 357, IOP Publishing, 2019, p. 012035.
- 573 [39] D. Zeng, S. Zhang, F. Chen, Y. Wang, Multi-scale cnn based garbage
574 detection of airborne hyperspectral data, *IEEE Access* 7 (2019) 104514–
575 104527.

- 576 [40] R. Barzegar, M. T. Aalami, J. Adamowski, Coupling a hybrid cnn-lstm
577 deep learning model with a boundary corrected maximal overlap discrete
578 wavelet transform for multiscale lake water level forecasting, *Journal of*
579 *Hydrology* 598 (2021) 126196.
- 580 [41] M. Panahi, N. Sadhasivam, H. R. Pourghasemi, F. Rezaie, S. Lee, Spa-
581 tial prediction of groundwater potential mapping based on convolutional
582 neural network (cnn) and support vector regression (svr), *Journal of Hy-*
583 *drology* 588 (2020) 125033.
- 584 [42] X. Guo-yan, Z. Jin, S. Cun-you, H. Wen-bin, L. Fan, Combined hydro-
585 logical time series forecasting model based on cnn and mc, *Computer*
586 *and Modernization* (2019) 23.
- 587 [43] D. Hussain, T. Hussain, A. A. Khan, S. A. A. Naqvi, A. Jamil, A deep
588 learning approach for hydrological time-series prediction: A case study
589 of gilgit river basin, *Earth Science Informatics* 13 (2020) 915–927.
- 590 [44] T. Tu, K. Ishida, A. Ercan, M. Kiyama, M. Amagasaki, T. Zhao, Hybrid
591 precipitation downscaling over coastal watersheds in japan using wrf and
592 cnn, *Journal of Hydrology: Regional Studies* 37 (2021) 100921.
- 593 [45] F. R. Adaryani, S. J. Mousavi, F. Jafari, Short-term rainfall forecast-
594 ing using machine learning-based approaches of pso-svr, lstm and cnn,
595 *Journal of Hydrology* 614 (2022) 128463.

- 596 [46] Y. Wang, Z. Fang, H. Hong, L. Peng, Flood susceptibility mapping
597 using convolutional neural network frameworks, *Journal of Hydrology*
598 582 (2020) 124482.
- 599 [47] C. M. Song, Data construction methodology for convolution neural
600 network based daily runoff prediction and assessment of its applicability,
601 *Journal of Hydrology* 605 (2022) 127324.
- 602 [48] Y. Li, W. Wang, G. Wang, Q. Tan, Actual evapotranspiration esti-
603 mation over the tuojiang river basin based on a hybrid cnn-rf model,
604 *Journal of Hydrology* 610 (2022) 127788.
- 605 [49] S. Kabir, S. Patidar, X. Xia, Q. Liang, J. Neal, G. Pender, A deep
606 convolutional neural network model for rapid prediction of fluvial flood
607 inundation, *Journal of Hydrology* 590 (2020) 125481.

608 **Appendix A. The U-Net Model**

609 Computer vision techniques such as image segmentation has surged in
610 popularity in recent years, with applications in scene understanding, medical
611 image analysis, robotic perception, video surveillance, augmented reality, and
612 image compression among others [36]. Deep learning models such as Convo-
613 lutional Neural Networks (CNN) are being increasingly applied in environ-
614 mental sciences, e.g., air quality modeling [37], image classification [38, 39]
615 etc. In hydrological sciences, CNNs have been used for lake water level

616 forecasting [40], prediction of groundwater potential mapping [41], hydro-
617 logical time series forecasting modeling [42, 43], rainfall forecasting [44, 45],
618 flood susceptibility mapping [46], daily runoff prediction [47], evapotran-
619 spiration estimation [48], and rapid production of fluvial flood inundation
620 [49] among other applications. In this study, we approach understanding
621 human-meteorological drought(MD)interactions using large-scale (CONUS
622 scale) maps/images, making CNNs ideal candidates for our objectives. We
623 used U-Net, which is a deep learning model used that was developed for im-
624 age segmentation to learn relationships between meteorological droughts and
625 search interest. Inputs to the model are SPEI maps over the CONUS and
626 targets are Google SI maps over the CONUS.

627 *Appendix A.1. Model Architecture*

628 The U-Net is a convolutional neural network with an encoder-decoder
629 architecture. Our model architecture (Fig. A.13) has two encoder blocks.
630 Each encoder block has two convolutional layers followed by ReLU activa-
631 tion functions and one Max-pooling layer. The first encoder block captures
632 low-level features of the input images, e.g. edges, corners and textures. The
633 second encoder block builds on the first one by capturing higher level fea-
634 tures and patterns. A middle block consisting of two convolutional layers
635 and ReLU activation functions processes the high-level features captured by
636 the encoder blocks. There are two decoder blocks - the first one starts the
637 upsampling process to generate the output image. It consists of a transposed

638 convolutional layer (also called deconvolutional layer) followed by two convo-
639 lutional layers and corresponding ReLU activation layers. The first decoder
640 block combines the features from the middle block with the high level fea-
641 tures of the second encoder block. The second decoder block continues the
642 upsampling process by combining the features from the first decoder block
643 with the low-level features from the first encoder block. It has one trans-
644 posed convolutional layer followed by two 3x3 convolutional layers and one
645 1x1 convolutional layer to produce the final output image. In a broad sense,
646 this allows the model to skip connections, allowing information to flow di-
647 rectly from the encoder to the decoder blocks, helping the network preserve
648 finer features in the output image.

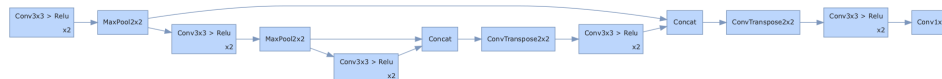


Figure A.13: Our custom U-Net Model Architecture (image generated with Hiddenlayer library).

649 *Appendix A.2. Model Training*

650 We split our training and testing data using an 80/20 ratio, so that 163
651 months of SPEI data and corresponding SI data were used for training and
652 41 months of data were used for testing. We trained six U-Net models on
653 the six different sets of SPEI images (as defined earlier). Starting from zero
654 months lag (0ml) to 5 months lag (5ml). These lags allow us to statistically
655 explore any temporal trends between meteorological drought events and an-

656 thropogenic response to these events (in terms of when people within our
657 study domain become interested in topics related to droughts). The training
658 process involved feeding input SPEI images and their corresponding SI labels
659 to the model and loss function, respectively. We used an adaptive moment
660 (ADAM) optimizer with a Mean Squared Error (MSE) loss, a batch size of
661 1 image, and 20 training epochs.

662 *Appendix A.3. Model Evaluation*

663 We evaluated models on the test set of 41 images. The output of the
664 U-Net models are probability maps that have the same shape as the input
665 image (i.e., the same spatial resolution as the SPEI images). These vectors
666 represent the probability of each pixel belonging to the target class (SI maps).
667 We then calculated the average R-squared scores for each model.